ChemPubSoc Europe

DOI: 10.1002/chem.201502809

CHEMISTRY A European Journal Full Paper

Photopharmacology

Light-Controlled Histone Deacetylase (HDAC) Inhibitors: Towards Photopharmacological Chemotherapy

Wiktor Szymanski,*[a, b] Maria E. Ourailidou,[c] Willem A. Velema,[a] Frank J. Dekker,*[c] and Ben L. Feringa*[a]

Abstract: Cancer treatment suffers from limitations that have a major impact on the patient's quality of life and survival. In the case of chemotherapy, the systemic distribution of cytotoxic drugs reduces their efficacy and causes severe side effects due to nonselective toxicity. Photopharmacology allows a novel approach to address these problems because it employs external, local activation of chemotherapeutic agents by using light. The development of photoswitchable histone deacetylase (HDAC) inhibitors as potential antitumor agents is reported herein. Analogues of the clinically used chemotherapeutic agents vorinostat, panobinostat, and belinostat were designed with a photoswitchable azobenzene moiety incorporated into their structure. The most promising compound exhibits high inhibitory potency in the thermodynamically less stable *cis* form and a significantly lower activity for the *trans* form, both in terms of HDAC activity and proliferation of HeLa cells. This approach offers a clear prospect towards local photoactivation of HDAC inhibition to avoid severe side effects in chemotherapy.

Introduction

Chemotherapy, besides radiotherapy and surgery, is one of the crucial elements of cancer treatment.[1] It relies on the systemic administration of cytotoxic antineoplastic agents, which are infamous for their severe side effects.[2] Efforts towards targeted delivery of chemotherapeutics are often insufficient, and therefore, the lack of drug selectivity remains a major problem in care for cancer patients.[3] Ineffective cancer treatment causes unrelenting emotional and societal burdens to the patients and their environment and also has a massive economic impact.[4] In the case of cancer types that warrant localized treatment, high spatiotemporal control over the activity of the drug, that is, the possibility to externally modulate the potency of the chemotherapeutic agent, would allow the systemic side effects to be avoided by minimizing the concentration of active compound outside the area of treatment, thereby tremendously increasing the quality of the patient's life.[5]

Photopharmacology[6,7] aims at using light as an external, noninvasive control element to modulate drug activity (Figure 1). Light can be delivered with very high spatiotemporal precision, with a wide range of intensities and wavelengths[8,9] and very limited effects on the patient's body. From a medicinal chemistry perspective, photopharmaceuticals are developed by the incorporation of photoresponsive molecular switches into existing drugs to enable alteration of their biological properties upon light irradiation.[8–10] Photoswitching is reversible by irradiation with light of different wavelengths or in a thermal process.[11] Recent examples of bioactive compounds with photomodulated potency include photocontrolled ion-channel blockers,[12] antibiotics,[13] and enzyme inhibitors.[14] However, successful examples for switch-on chemotherapeutics are currently lacking.

For a possible therapeutic application, the potential photopharmaceuticals must fulfill a number of criteria. First, they must show high potency that is at least comparable with the parent, clinically useful drug that inspired their design. Second, the difference in activity between the inactive and active states should be sufficiently large to allow for "off–on" switching of their activity under physiological conditions. Finally, the thermodynamically less stable form should show higher biological activity, preferably with a known mechanism of toxicity, to enable precise local activation, as presented in Figure 1. Photopharmaceuticals have been described that meet some of these requirements, that is, high potency,[15] >20 times difference in activity,[16] and enhanced potency for the unstable state.[13] However, fulfilling all of these criteria in one molecule

[a] *Dr. W. Szymanski,[+] Dr. W. A. Velema, Prof. Dr. B. L. Feringa*
Centre for Systems Chemistry, Stratingh Institute for Chemistry
University of Groningen, Nijenborgh 4
9747 AG, Groningen (The Netherlands)
E-mail: b.l.feringa@rug.nl

[b] *Dr. W. Szymanski[+]*
Department of Radiology, University of Groningen
University Medical Center Groningen Hanzeplein 1
9713 GZ, Groningen (The Netherlands)
E-mail: w.szymanski@umcg.nl

[c] *M. E. Ourailidou,[+] Prof. Dr. F. J. Dekker*
Department of Pharmaceutical Gene Modulation
University of Groningen, Antonius Deusinglaan 1
9713 AV Groningen (The Netherlands)
E-mail: f.j.dekker@rug.nl

[+] *These authors contributed equally to this work.*

Supporting information for this article is available on the WWW under http://dx.doi.org/10.1002/chem.201502809.

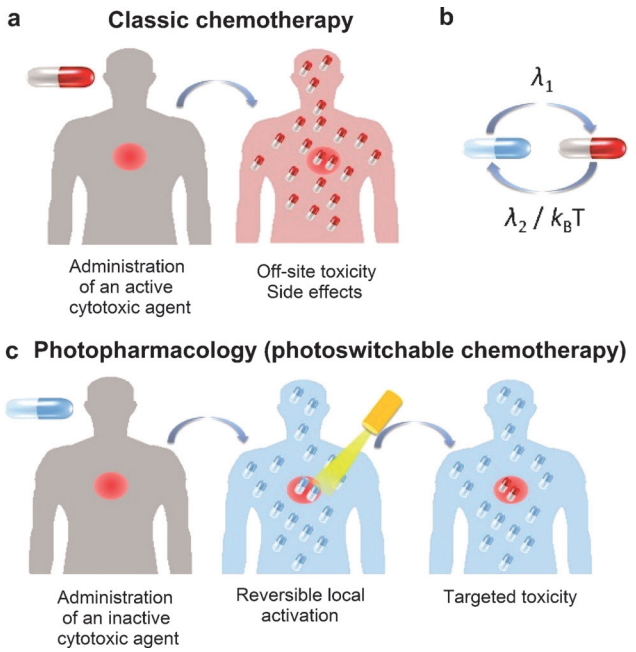

Figure 1. Comparison of the principles behind classic chemotherapy (a) and high-precision photopharmacological chemotherapy (b,c). The reversible photoswitching between the inactive (blue) and active (red) chemotherapeutic agent (b) allows for local activation of the drug and permits its use at elevated concentrations, without systemic side effects (c).

remains a major challenge and is crucial for the development of a clinically useful, photoactivated drug.

To demonstrate the viability of this novel approach with the ultimate goal of photoresponsive chemotherapy, we have chosen histone deacetylases (HDACs) as a pharmacological target. The function of HDACs is the deacetylation of ε-acetylated lysine residues on histone tails to restore the positive charge of the histones and their electrostatic interactions with DNA, leading to condensed and transcriptionally silent chromatin structures.[17]

The HDAC family members are categorized into four classes (I–IV), based on their primary structure, size, and sequence homology to the respective yeast enzymes.[18,19] The mechanism of deacetylase activity is zinc dependent for classes I (HDAC1–3 and 8); II, which is subdivided into classes IIa (HDAC4, 5, 7, and 9) and IIb (HDAC6 and 10); and IV, and nicotinamide adenine dinucleotide (NAD^+) dependent for class III. As epigenetic regulators of both histone and non-histone proteins,[20] HDACs play a pivotal role in a vast array of biological processes, including DNA repair, cell differentiation, proliferation, and apoptosis. As a result, alterations in expression or mutations of genes encoding for HDACs can lead to aberrant gene transcription, disruption of cell homeostasis, and subsequently to tumorigenesis.[21–23] Recent evidence demonstrates that individual HDACs are strongly associated with neurodegenerative[24–26] and inflammatory diseases,[27,28] tissue fibrosis, and metabolic disorders.[21]

The link between abnormal HDAC activity and cancer initiation and progression is best shown in classes I, II, and IV.[21] A large variety of natural and synthetic compounds have been reported as potential agents for cancer prevention or treatment of different stages of several tumor types. Depending on their structure, they can be categorized to hydroxamic acids, cyclic peptides, benzamides, and short-chain fatty acids.[20,22] To date, there are 11 different HDAC inhibitors (HDACis) undergoing clinical trials as monotherapy or in combination with other antitumor approaches in cancer patients.[29] The most successful inhibitors, so far, proved to be the hydroxamic acid type pan-HDACis, from which three have obtained US Food and Drug Administration (FDA) approval for clinical use: vorinostat (SAHA), panobinostat, and belinostat.[30] These compounds nonselectively inhibit class I, II, and IV HDACs with a nanomolar-scale potency[31] and are successfully applied as chemotherapeutic agents for the treatment of hematologic malignancies.[30,32–34] However, despite significant efforts, the specific HDACs responsible for the clinical effects of these successful inhibitors have not been elucidated as yet.[31,34]

The crystal structure of human deacetylase-like protein (HDLP) with SAHA shows that SAHA binds inside the catalytic pocket by inserting the chain into the enzymatic channel (Figure 2).[35] The hydroxamic acid interacts with the zinc cation at the polar bottom part and also forms hydrogen bonds with catalytic residues. Moreover, the aliphatic chain makes van der Waals interactions with residues at the hydrophobic part of the pocket, whereas the cap group serves in packing the inhibitor at the rim of the active site.

The insertion of SAHA into the channel of the deacetylase and the flexibility of the aliphatic chain suggest that the inhibitory activity may be controlled by changes in length, shape, and substituents of the molecule. During the studies reported herein, a patent was published that demonstrated an increased activity for the *cis* isomers of azobenzene–benzamide-type HDAC inhibitors.[36] Despite their potential clinical relevance, compounds of this class lack the high toxicity for cancer cells generally reported for hydroxamic-acid-type HDAC inhibitors. Therefore, we have chosen to employ the clinically approved inhibitors SAHA, panobinostat, and belinostat as starting points for the design of photoswitchable HDACis, as potential photocontrolled chemotherapeutic agents for improved, safer cancer therapy with less severe side effects. We aimed to design a potent compound that would show high activity in the thermodynamically unstable *cis* state and very little cytotoxicity in the stable *trans* state.

We have chosen the azobenzene photoswitch as a photoresponsive element that, when incorporated into the structure of chemotherapeutic agents, should provide control over their activity with light. Azobenzene molecules can be switched, usually by using UV irradiation, from a flat, *trans* isomer to the bent *cis* isomer (Figure 3a).[11] The latter, which is thermodynamically less stable than the former, will switch back to the initial state over time (Figure 3a). This reverse process can also be achieved by using visible-light irradiation. Importantly, the two forms show major differences in their shape and polarity, and therefore, light-induced isomerization will result in switching of the properties of an azobenzene-modified drug, which may consequently change the drug's biological activity.

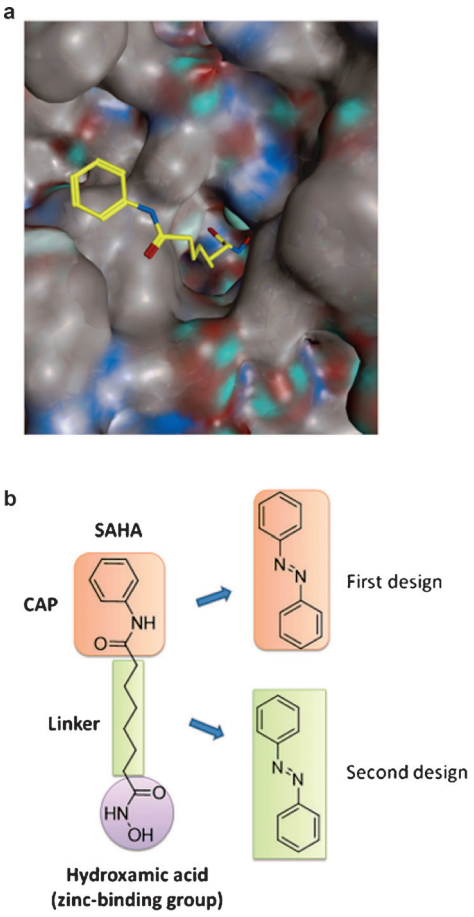

Figure 2. Structural design of photoswitchable HDAC inhibitors. a) Crystal structure of HDLP from *Aquifex aeolicus* in complex with SAHA. The aliphatic chain is inserted into the enzymatic channel, in which the hydroxamic group interacts with the zinc cation, leaving the cap at the rim of the catalytic pocket. The picture was adapted from PDB file 1C3S.[35] b) Molecular design of photoswitchable SAHA analogues, with the azobenzene moiety introduced into the cap (first design) or the linker region (second design).

Azobenzene photochromes with different properties have been used in photopharmacological projects due to their easy preparation, efficient photoswitching, and low rate of photobleaching.[8,9] Their electronic properties determine the absorption maxima and the half-lives of the *cis* isomers. Accordingly, azobenzenes with various substitution patterns were included in our newly designed inhibitors to optimize their photophysical properties and HDAC inhibition with respect to potency and selectivity. We also used a new class of tetra-*ortho*-substituted azobenzenes that could be photoisomerized by using visible light (up to $\lambda = 650$ nm), which allowed for lower toxicity and deeper tissue penetration.[37,38]

Results and Discussion

Two distinct approaches were taken in the molecular design of photoswitchable HDACi. In the first one (compounds **1**–**7**; Figure 3b), the photoswitches were introduced into the cap moiety of the SAHA molecule (Figure 2b). To systematically study the influence of the substitution pattern on the photochemical and pharmacological properties of the obtained photocontrolled chemotherapeutic agents, all possible attachments of azobenzene to SAHA (*para* (**1**), *meta* (**2**), and *ortho* (**3**)) were evaluated. Additionally, a *para*-MeO substituent was introduced into the terminal aromatic ring in compounds **4** and **5**, in an attempt to increase the *cis* content in the irradiated samples, as described for other azobenzenes.[39] The influence of the length of the aliphatic chain in the SAHA core was tested with compound **6**, which was a shortened homologue of compound **2**. Finally, we studied visible-light-switchable compound **7** to evaluate the possibility of using higher and more biocompatible wavelengths of light for the photocontrol of bioactivity.

In the second approach (compounds **8**–**12**), the linker part of the inhibitor (Figure 2b) was modified because it was more tightly embedded within the protein. We hypothesized that introducing a photoswitch into this part of the SAHA molecule would lead to increased photocontrol over binding because one of the photoisomeric forms should fit the tunnel better than another. Compounds **8**, **9**, **10**, and **11** were designed to test this hypothesis. In compound **9**, an additional benzyl moiety was introduced to mimic the cap in the SAHA molecule (Figure 2b). Homologous compounds **10** and **11** were prepared to test the influence of the inhibitor's flexibility and linker length in comparison to **8** and **9**. Finally, inspired by the structure of two known clinically approved inhibitors, belinostat and panobinostat,[40] we introduced a double bond into the linker part of compound **12**.

The biological activity assay (see below) we performed was based on the addition of the respective compound as a stock solution in DMSO to a buffered solution of enzyme and, after 1 h incubation at RT, measurement of the conversion of a profluorogenic substrate.[41] Therefore, two photochemical properties of the inhibitors are of importance: the content of *cis* isomer obtained upon irradiation in DMSO and the half-life of the thermodynamically unstable *cis* isomer under the assay conditions (Figure 3c and d, respectively). The latter value is also crucial for photopharmacological applications (Figure 1), in which one would envision the use of *cis*–*trans* isomerization for slow auto-inactivation of compounds that have been locally activated.

All of the compounds show a satisfactory photostationary state (PSS, $>76\%$, defined as the content of *cis* isomer, at equilibrium, under the $\lambda = 365$ nm light irradiation at ≈ 2 mg mL^{-1}) in DMSO (Figure 3c). In the isomeric series **1**–**3**, the lowest PSS was obtained for the *meta*-substituted compound and the highest (95%) for the *para* isomer. The introduction of methoxy substituents in compounds **4** and **5** indeed allowed the PSS to be increased with respect to parent structures **1** and **2** (from 95 (**1**) and 83% (**3**) to 97 (**4**) and 95% (**5**)). With compound **7**, we were able to achieve 78% PSS by using blue light ($\lambda = 400$ nm) and 61% PSS by using green light ($\lambda = 530$ nm), which is in line with similar tetra-*ortho*-substituted systems,[37,38] and permits the switching of these compounds with visible light. For all *para*-alkoxy-substituted compounds, **8**–**12**, a high PSS was reached ($>92\%$).

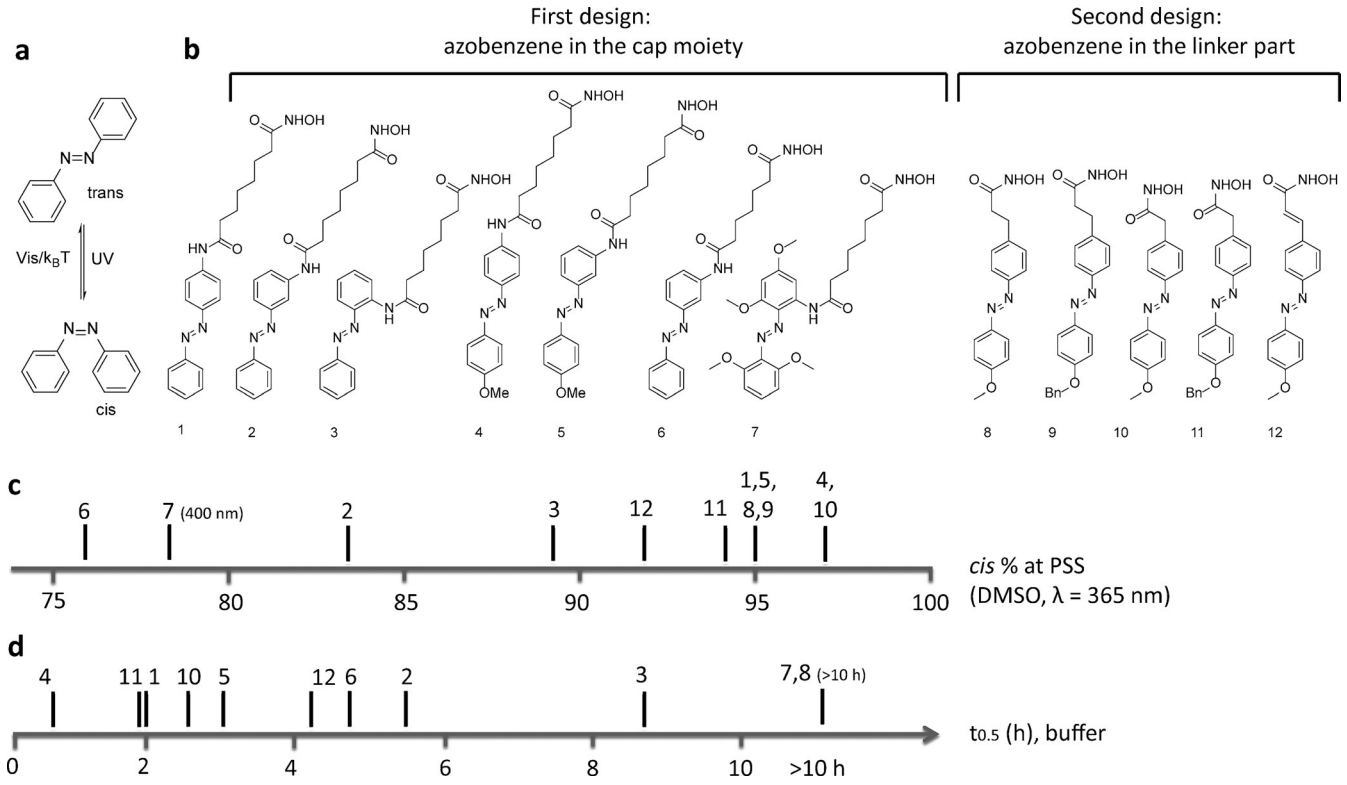

Figure 3. Structure and photochemical properties of compounds **1**–**12** (for synthetic procedures and analytical data, see the Supporting Information). a) Reversible photochromism of an azobenzene molecule. b) Molecular structure of compounds **1**–**12**. c) The content (%) of the *cis* isomer in the photostationary state in DMSO, $\lambda_{irrad} = 365$ nm, as determined by ^{1}H NMR spectroscopy. d) Half-life (in the dark, at room temperature) for the thermodynamically unstable *cis* isomer, as determined by UV/Vis spectroscopy at room temperature in the HDAC assay buffer with 1 vol% DMSO.

By changing the substitution pattern, we can control the half-life of the inhibitors from minutes to hours, which is of key importance in designing potential chemotherapeutics that are meant, after photoactivation, to auto-inactivate in the patient's body (Figure 3d). Very high stability was observed for compound **7**, which is in line with earlier studies on tetra-*ortho*-substituted systems.[38]

Importantly, all of the studied compounds are stable towards reduction in the cellular environment, as shown by repeating switching cycles[42–44] in buffer in the presence of 10 mM glutathione (GSH; Figure S5 in the Supporting Information), which is the highest concentration of GSH found in cells.[45]

Compounds **1**–**12** were initially screened for their inhibitory potency of crude enzyme activity (Figures S11 and S12 in the Supporting Information) by using a published protocol.[41] Nuclear extracts from HeLa cells were used as a source of class I HDACs.[46] Gratifyingly, for the *meta*-substituted compounds **2** and **5**, we observed even higher potency than that of the original drug. A significant difference in activity between the two isomeric forms, which is crucial for photopharmacological applications, was apparent in the *meta*- and *ortho*-substituted compounds, among which compound **3** showed the highest *trans*/*cis* activity ratio (approximately 3×). Compounds of the second design (**8**–**12**; Figure 3), turned out to be less potent than those from the first design. However, in all cases, stronger HDAC inhibition was observed for the *cis* isomer, the potency of which increased from the micro- to nanomolar scale with the introduction of a second carbon in the chain.

We tested selected compounds for the inhibition of human recombinant class I HDACs (1–3 and 8) and HDAC6 (class IIb; Table 1 and Figure 4). The active form of compound **1** (*cis*, except for HDAC3) was less potent than SAHA, whereas compounds **2** and **3** showed a remarkable potency in their *trans* forms, with an IC_{50} value of 12 nM (15× more potent than SAHA) in HDAC2 for compound **2** and 7.7 nM in HDAC3 for compound **3**. The same profile was observed with the visible-light-switchable compound **7** (up to 12× more potent than SAHA in HDAC2). The highest difference in IC_{50} values between the two isomers was observed for compound **3** (10× for HDAC3), whereas the same ratio was moderate for compounds **1** and **2** and relatively good for compound **7** (almost 6× for HDAC3). Considerable inhibitory potency was also observed for compound **6** (*trans* form), which was the shorter analogue of **2**, but the *cis*/*trans* activity difference was significant only in the case of HDAC3. Despite promising results from the HeLa nuclear extracts (Figure S11 in the Supporting Information), the potency of *trans*-**5** in HDACs1-3 was comparable to that of SAHA and the *cis*/*trans* activity ratio was rather small (Figure 4a).

In the second design, the most active form of the inhibitor is the less stable *cis* isomer, which is advantageous for photopharmacological applications (Figure 1). Compounds **8** and **12** proved to have lower potency than that of SAHA in HDACs1–3

Table 1. Inhibition of HDAC activity by photoswitchable SAHA, panobinostat, and belinostat analogues.

	IC_{50} [μM]									
	HDAC1		HDAC2		HDAC3		HDAC6		HDAC8	
	trans	*cis*	*trans*	*cis*	*trans*	*cis*	*trans*	*cis*	*trans*	*cis*
1	0.081 ± 0.012	0.045 ± 0.008	2.185 ± 0.327	0.401 ± 0.133	0.144 ± 0.052	0.335 ± 0.103	0.010 ± 0.002	0.048 ± 0.014	1.609 ± 0.423	0.777 ± 0.160
2	0.014 ± 0.006	0.035 ± 0.023	0.012 ± 0.002	0.056 ± 0.012	0.019 ± 0.009	0.022 ± 0.007	0.013 ± 0.003	0.047 ± 0.013	0.125 ± 0.025	0.087 ± 0.016
3	0.013 ± 0.003	0.057 ± 0.011	0.043 ± 0.010	0.185 ± 0.042	0.008 ± 0.002	0.073 ± 0.020	0.335 ± 0.105	0.210 ± 0.080	0.070 ± 0.022	0.320 ± 0.101
5	0.040 ± 0.010	0.047 ± 0.011	0.113 ± 0.020	0.098 ± 0.014	0.030 ± 0.011	0.067 ± 0.023	0.394 ± 0.083	0.151 ± 0.027	0.843 ± 0.204	0.445 ± 0.107
6	0.025 ± 0.011	0.024 ± 0.006	0.034 ± 0.004	0.045 ± 0.012	0.011 ± 0.003	0.096 ± 0.042	0.043 ± 0.011	0.082 ± 0.033	0.247 ± 0.057	0.099 ± 0.027
7	0.008 ± 0.002	0.050 ± 0.011	0.015 ± 0.003	0.091 ± 0.018	0.025 ± 0.006	0.061 ± 0.011	0.132 ± 0.041	0.198 ± 0.065	0.122 ± 0.036	0.095 ± 0.021
8	0.855 ± 0.196	0.137 ± 0.029	8.506 ± 2.331	0.444 ± 0.119	0.428 ± 0.086	0.094 ± 0.033	0.353 ± 0.088	0.190 ± 0.063	0.830 ± 0.149	1.313 ± 0.403
12	0.658 ± 0.141	0.080 ± 0.020	21.65 ± 8.095	0.555 ± 0.121	0.320 ± 0.115	0.071 ± 0.013	0.114 ± 0.024	0.110 ± 0.039	0.237 ± 0.047	0.462 ± 0.137

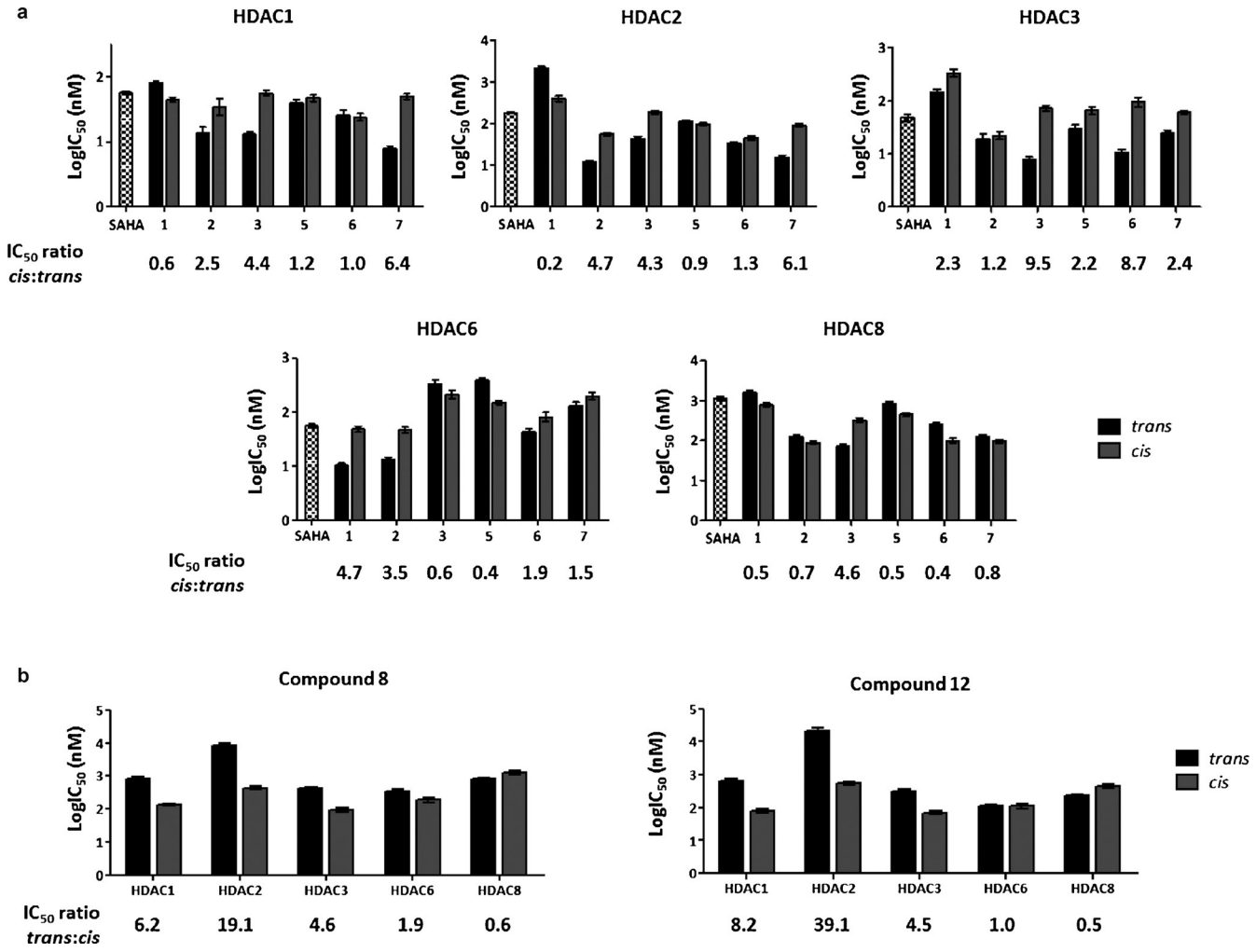

Figure 4. Inhibition of human recombinant class I HDACs and HDAC6 (class IIb). Inhibitory potency of *trans* (black) and *cis* (gray) forms of selected compounds of the a) first and b) second designs. The corresponding IC_{50} ratios of the two isomers are also reported. The log IC_{50} values are presented as mean values of three independent measurements with their respective standard deviations.

(Table 1 and Figure 4b). However, we were delighted to observe a large increase in the IC_{50} ratio between the *trans* and *cis* isomers in the case of HDAC2 (19× for inhibitor **8** and nearly 40× for **12**; Figure 5b). Importantly, both compounds in the active (*cis*) state showed inhibition in the same concentration range as that of SAHA (IC_{50} = 0.44 μM for **8** and 0.56 μM for **12** vs. 0.18 μM for SAHA).

Interestingly, opposite activity results, compared with those for HDACs1–3, were obtained for HDAC8, since the potency of all inhibitors (including SAHA) was dramatically reduced (Table 1 and Figure 4a and b). This can be explained by structural and sequence alignments of class I HDACs, which reveal a particularly malleable active site for HDAC8.[47] Compound *trans*-**3** was found to be more active (IC_{50} = 70 nM, 16× more

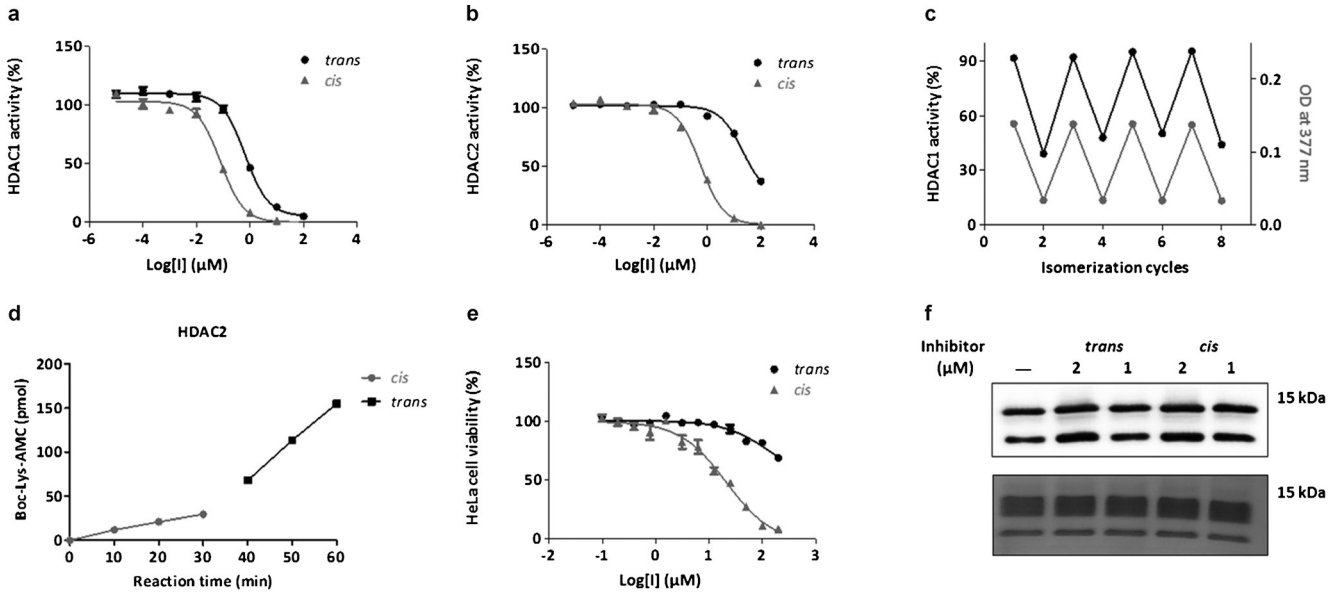

Figure 5. Studies on the performance of compound **12**. The IC_{50} curves in a) HDAC1 and b) HDAC2 recombinant enzymes of *trans* and *cis* forms of the inhibitor. c) Inhibition of HDAC1 activity with 50 nM of inhibitor **12** (black) and reversible photochromism (gray) after 4 isomerization cycles. d) In situ photoisomerization of **12**, after 30 min of incubation of the *cis* form (1 μM) with HDAC2, with white light. The formation of product was monitored at the indicated times. e) HeLa cell viability was measured after 16 h of incubation with various concentrations of each isomeric form of the inhibitor. f) On-blot luminescence detection and Coomassie Blue staining of acetylated histones (4 μg) after 16 h incubation with 1 and 2 μM of *cis*- and *trans*-**12** by using the anti-acetyl lysine antibody. a)–e) The data are presented as mean values of three independent measurements with their respective standard deviations.

potent than SAHA) and exhibited the biggest difference in potency (compared with the *cis* form) for HDAC8 inhibition.

Moreover, we examined the activity of selected compounds against HDAC6, which is an isoform with a critical role in tumorigenesis and cancer cell metastasis.[48] A considerable inhibitory potency was achieved in the case of the *trans* isomers of **1** and **2**; the *cis* form was comparable to the reference compound (Table 1 and Figure 4a and b).

The experiments described above were aimed at selecting the optimal photocontrolled HDACi for selective chemotherapy. Compound **12** fulfills all criteria described in the Introduction, that is, high potency of the *cis* state (HDAC2 IC_{50} = 0.56 μM) with a very large difference from the *trans* state. Furthermore, we tested if its reversible photochromism (switching back and forth between the isomers) was reflected in reversible changes in activity. To that end, compound **12** was tested for HDAC1 inhibition by using cycles of *trans*–*cis* isomerization of the same stock solution. The residual HDAC1 activity had a reversible profile and dropped from 90 (*trans*) to 50% (*cis*) after each isomerization (Figure 5c). This experiment excludes the possibility that irradiation results in the irreversible formation of compounds with altered inhibitory activity against HDACs.

Next, we evaluated the possibility of using light to change the activity of compound **12** in situ during the HDAC2 enzymatic activity assay. After 30 min of incubation with the more active *cis* form, white-light irradiation was applied to the enzymatic reaction to induce switching to the less active *trans* form. In line with our expectations, the rate of product formation was considerably increased (Figure 5d) due to the poor inhibitory potency of *trans*-**12**. This experiment confirms that light can be used in a biological setting to change the activity of photoswitchable HDAC inhibitors presented herein.

Finally, we elucidated the global cytotoxic activity of photoswitchable HDACi and the extent to which it could be photocontrolled. Chosen compounds were incubated, in both isomeric forms, with HeLa cells for 16 h at 37 °C, followed by measurement of cell viability (Figure S33 in the Supporting Information). In line with the results obtained for recombinant enzymes, the most promising results came from compound **12**, for which the *cis* form was significantly more toxic to the HeLa cervical cancer cells than the *trans* form (Figure 5e). At 100 μM, nearly full selectivity is obtained: the *cis* isomer kills almost all cells, whereas the *trans* isomer leaves almost all cells intact. This selectivity is remarkable, since the half-life of *cis*-**12** at 37 °C is relatively short (67 min). Moreover, both isomers resulted in increased histone acetylation (mainly histone H4) at concentrations of around 2 μM (Figure 5f), which indicated inhibition of intracellular HDAC activity. Because **12** is the only inhibitor prone to undergo conjugate addition (Figure 3a), possible attack from nucleophilic residues of cellular proteins may lead to irreversible inhibition. We observed, however, competitive inhibition (Lineweaver–Burk analysis; Figure S19 in the Supporting Information), which proved noncovalent binding to HDACs.

Conclusion

We presented herein the development of potential chemotherapeutic agents, the activity of which on their molecular targets could be externally controlled with light. Around the azobenzene photoswitchable moiety, inhibitors were designed that

were structurally related to the clinically approved HDAC inhibitors SAHA, panobinostat, and belinostat. The inhibitors were optimized towards high potency and pronounced inhibitory activity differences between the more active, thermodynamically less stable *cis* isomer and the less active *trans* isomer.

Notably, the introduction of the photoswitchable moiety did not compromise the HDAC inhibitory activity because some of the compounds showed potencies comparable, or even superior, to that of the original SAHA drug. By changing the substitution pattern of the azobenzene, we were able to strongly influence not only the potency for different HDACs, but also the growth of HeLa cervical cancer cells. Favorably, it also enabled the control of other important features of the photocontrolled inhibitor, such as the PSS, λ_{max}, and *cis* isomer half-life in aqueous medium.

The most exciting results were achieved with inhibitor **12**, which showed many characteristics of a privileged photocontrolled chemotherapeutic agent: high potency (in selected HDACs comparable to SAHA), very high difference in activity between the photoisomers on isolated enzymes (up to 39× for HDAC2) and whole cells, stable photoswitching, and stability against GSH reduction. Importantly, the photochemically accessible, less stable *cis* isomer of **12** was the one that showed much higher inhibitory potency, which was in line with the ultimate applications envisioned in Figure 1. In these applications, one can envision the use of visible light for inactivation of the drug outside the site of action. Alternatively, advantage could be taken of the relatively short half-life of this isomer in aqueous buffer (67 min), which would allow for relatively fast auto-inactivation of the drug outside the irradiated area.

Herein, we provided proof of concept that the development of photoswitchable inhibitors for a range of HDACs, in particular HDAC2, was feasible and that this photoswitching was also reflected in a change in cytotoxicity in HeLa cells. This creates a perspective towards several clinical applications. The use of the photoreactive agents presented herein, which require UV irradiation, would currently be limited to topical or intraoperative chemotherapy, such as use in the hyperthermic intraperitoneal chemotherapy (HIPEC) procedure.[49] However, we have also shown that significant activity can be obtained with visible-light switchable compound **7**, and due to the low toxicity and higher tissue penetration of visible light, this offers a promising approach towards fully noninvasive photopharmacology. Employing such compounds[42,43,50] provides prospects for future precision chemotherapy, combining molecular tracers for tumor imaging with chemotherapeutic agents that can be photoactivated with high spatiotemporal precision.

Acknowledgements

Financial support from the Netherlands Organization for Scientific Research (NWO-CW), the Royal Netherlands Academy of Arts and Sciences (KNAW), the European Research Council (ERC advanced grant 227897), and the Ministry of Education, Culture and Science (Gravitation Program 024.001.035) to B.L.F. is gratefully acknowledged. This work was also financially supported by a VIDI grant (016.122.302) from the Netherlands Organization for Scientific Research and an ERC starting grant (309782) from the European Union to F.J.D.

Keywords: cancer · cytotoxicity · drug design · inhibitors · photochemistry

[1] R. Siegel, C. DeSantis, K. Virgo, K. Stein, A. Mariotto, T. Smith, D. Cooper, T. Gansler, C. Lerro, S. Fedewa, C. Lin, C. Leach, R. Cannady, H. Cho, S. Scoppa, M. Hachey, R. Kirch, A. Jemal, E. Ward, *Ca-Cancer J. Clin.* **2012**, *62*, 220 – 241.
[2] A. Ihbe-Heffinger, B. Paessens, K. Berger, M. Shlaen, R. Bernard, C. von Schilling, C. Peschel, *Supportive Care Cancer* **2013**, *21*, 1665 – 1675.
[3] Y. H. Bae, K. Park, *J. Controlled Release* **2011**, *153*, 198 – 205.
[4] M. J. Hassett, A. J. O'Malley, J. R. Pakes, J. P. Newhouse, C. C. Earle, *J. Natl. Cancer Inst.* **2006**, *98*, 1108 – 1117.
[5] M. J. Hansen, W. A. Velema, G. de Bruin, H. S. Overkleeft, W. Szymanski, B. L. Feringa, *ChemBioChem* **2014**, *15*, 2053 – 2057.
[6] W. A. Velema, W. Szymanski, B. L. Feringa, *J. Am. Chem. Soc.* **2014**, *136*, 2178 – 2191.
[7] I. Tochitsky, A. Polosukhina, V. E. Degtyar, N. Gallerani, C. M. Smith, A. Friedman, R. N. Van Gelder, D. Trauner, D. Kaufer, R. H. Kramer, *Neuron* **2014**, *81*, 800 – 813.
[8] W. Szymanski, J. M. Beierle, H. A. V. Kistemaker, W. A. Velema, B. L. Feringa, *Chem. Rev.* **2013**, *113*, 6114 – 6178.
[9] A. A. Beharry, G. A. Woolley, *Chem. Soc. Rev.* **2011**, *40*, 4422 – 4437.
[10] G. Mayer, A. Heckel, *Angew. Chem. Int. Ed.* **2006**, *45*, 4900 – 4921; *Angew. Chem.* **2006**, *118*, 5020 – 5042.
[11] H. M. Dhammika Bandara, S. C. Burdette, *Chem. Soc. Rev.* **2012**, *41*, 1809 – 1825.
[12] J. Broichhagen, M. Schönberger, S. C. Cork, J. A. Frank, P. Marchetti, M. Bugliani, A. M. Shapiro, S. Trapp, G. A. Rutter, D. J. Hodson, D. Trauner, *Nat. Commun.* **2014**, *5*, 5116.
[13] W. A. Velema, J. P. van der Berg, M. J. Hansen, W. Szymanski, A. J. M. Driessen, B. L. Feringa, *Nat. Chem.* **2013**, *5*, 924 – 928.
[14] B. Reisinger, N. Kuzmanovic, P. Löffler, R. Merkl, B. König, R. Sterner, *Angew. Chem. Int. Ed.* **2014**, *53*, 595 – 598; *Angew. Chem.* **2014**, *126*, 606 – 609.
[15] J. Broichhagen, I. Jurastow, K. Iwan, W. Kummer, D. Trauner, *Angew. Chem. Int. Ed.* **2014**, *53*, 7657 – 7660; *Angew. Chem.* **2014**, *126*, 7788 – 7792.
[16] C. Falenczyk, M. Schiedel, B. Karaman, T. Rumpf, N. Kuzmanovic, M. Grøtli, W. Sippl, M. Jung, B. König, *Chem. Sci.* **2014**, *5*, 4794 – 4799.
[17] S. Y. Roth, J. M. Denu, C. D. Allis, *Annu. Rev. Biochem.* **2001**, *70*, 81 – 120.
[18] I. V. Gregoretti, Y. M. Lee, H. V. Goodson, *J. Mol. Biol.* **2004**, *338*, 17 – 31.
[19] K. V. Woan, E. Sahakian, E. M. Sotomayor, E. Seto, A. Villagra, *Immunol. Cell. Biol.* **2012**, *90*, 55 – 65.
[20] S. Minucci, P. G. Pelicci, *Nat. Rev. Cancer* **2006**, *6*, 38 – 51.
[21] J. Tang, H. Yan, S. Zhuang, *Clin. Sci.* **2013**, *124*, 651 – 662.
[22] M. Dokmanovic, C. Clarke, P. A. Marks, *Mol. Cancer Res.* **2007**, *5*, 981 – 989.
[23] S. Ropero, M. Esteller, *Mol. Oncol.* **2007**, *1*, 19 – 25.
[24] K. J. Falkenberg, R. W. Johnstone, *Nat. Rev. Drug Discovery* **2014**, *13*, 673 – 691.
[25] C. Simões-Pires, V. Zwick, A. Nurisso, E. Schenker, P. A. Carrupt, M. Cuendet, *Mol. Neurodegener.* **2013**, *8*, 7.
[26] K. Xu, X. L. Dai, H. C. Huang, Z. F. Jiang, *Oxid. Med. Cell. Longev.* **2011**, 143269.
[27] F. J. Dekker, T. van den Bosch, N. I. Martin, *Drug Discovery Today* **2014**, *19*, 654 – 660.
[28] M. A. Halili, M. R. Andrews, M. J. Sweet, D. P. Fairlie, *Curr. Top. Med. Chem.* **2009**, *9*, 309 – 319.
[29] A. C. West, R. W. Johnstone, *J. Clin. Invest.* **2014**, *124*, 30 – 39.
[30] M. Mottamal, S. Zheng, T. L. Huang, G. Wang, *Molecules* **2015**, *20*, 3898 – 3941.
[31] P. Atadja, *Cancer Lett.* **2009**, *280*, 233 – 241.
[32] O. Khan, N. B. La Thague, *Nat. Clin. Pract. Oncol.* **2008**, *5*, 714 – 726.
[33] P. A. Marks, R. Breslow, *Nat. Biotechnol.* **2007**, *25*, 84 – 90.
[34] P. Chun, *Arch. Pharmacal Res.* **2015**, *38*, 933 – 949.

[35] M. S. Finnin, J. R. Donigian, A. Cohen, V. M. Richon, R. A. Rifkind, P. A. Marks, R. Breslow, N. P. Pavletich, *Nature* **1999**, *401*, 188 – 193.
[36] R. Mazitschek, B. Ghosh, J. A. Hendricks, S. Reis, S. J. Haggarty, Photoswitchable hdac inhibitors. WO2014160221 A1, **2014**.
[37] S. Samanta, A. A. Beharry, O. Sadovski, T. M. McCormick, A. Babalhavaeji, V. Tropepe, G. A. Woolley, *J. Am. Chem. Soc.* **2013**, *135*, 9777 – 9784.
[38] D. Bléger, J. Schwarz, A. M. Brouwer, S. Hecht, *J. Am. Chem. Soc.* **2012**, *134*, 20597 – 20600.
[39] W. Szymanski, B. Wu, C. Poloni, D. B. Janssen, B. L. Feringa, *Angew. Chem. Int. Ed.* **2013**, *52*, 2068 – 2072; *Angew. Chem.* **2013**, *125*, 2122 – 2126.
[40] J. Tan, S. Cang, Y. Ma, R. L. Petrillo, D. Liu, *J. Hematol. Oncol.* **2010**, *3*, 5.
[41] D. Wegener, F. Wirsching, D. Riester, A. Schwienhorst, *Chem. Biol.* **2003**, *10*, 61 – 68.
[42] S. Samanta, C. Qin, A. J. Lough, G. A. Woolley, *Angew. Chem. Int. Ed.* **2012**, *51*, 6452 – 6455; *Angew. Chem.* **2012**, *124*, 6558 – 6561.
[43] S. Samanta, T. M. McCormick, S. K. Schmidt, D. S. Seferos, G. A. Woolley, *Chem. Commun.* **2013**, *49*, 10314 – 10316.
[44] E. Kosower, H. Kanety-Londner, *J. Am. Chem. Soc.* **1976**, *98*, 3001 – 3007.
[45] H. R. López-Mirabal, J. R. Winther, *Biochim. Biophys. Acta Mol. Cell Res.* **2008**, *1783*, 629 – 640.
[46] A. J. M. de Ruijter, A. H. van Gennip, H. N. Caron, S. Kemp, A. B. van Kuilenburg, *Biochem. J.* **2003**, *370*, 737 – 749.
[47] J. R. Somoza, R. J. Skene, B. A. Katz, C. Mol, J. D. Ho, A. J. Jennings, C. Luong, A. Arvai, J. J. Buggy, E. Chi, J. Tang, B. C. Sang, E. Verner, R. Wynands, E. M. Leahy, D. R. Dougan, G. Snell, M. Navre, M. W. Knuth, R. V. Swanson, D. E. McRee, L. W. Tari, *Structure* **2004**, *12*, 1325 – 1334.
[48] G. I. Aldana-Masangkay, K. M. Sakamoto, *J. Biomed. Biotechnol.* **2011**, 875824.
[49] K. Turaga, E. Levine, R. Barone, R. Sticca, N. Petrelli, L. Lambert, G. Nash, M. Morse, R. Adbel-Misih, H. R. Alexander, F. Attiyeh, D. Bartlett, A. Bastidas, T. Blazer, Q. Chu, K. Chung, L. Dominguez-Parra, N. J. Espat, J. Foster, K. Fournier, R. Garcia, M. Goodman, N. Hanna, L. Harrison, R. Hoefer, M. Holtzman, J. Kane, D. Labow, B. Li, A. Lowy, P. Mansfield, E. Ong, C, Pameijer, J. Pingpank, M. Quinones, R. Royal, G. Salti, A. Sardi, P. Shen, J. Skitzki, J. Spellman, J. Stewart, J. Esquivel, *Ann. Surg. Oncol.* **2014**, *21*, 1501 – 1505.
[50] Y. Yang, R. P. Hughes, I. Aprahamian, *J. Am. Chem. Soc.* **2012**, *134*, 15221 – 15224.

Received: July 17, 2015
Published online on September 29, 2015